A simple model of the turnover of organic carbon in a soil profile: model test, parameter identification and sensitivity

Elsa Coucheney[1], Anke M. Herrmann[1], Nicholas Jarvis[1]

[1]Department of Soil and Environment, Swedish University of Agricultural Sciences, Lennart Hjelms väg 9, 756 51 Uppsala, Sweden

Correspondence to: Elsa Coucheney (elsa.coucheney@slu.se)

Abstract. Simulation models are potentially useful tools to test our understanding of the processes involved in the turnover of soil organic carbon (SOC) and to evaluate the role of management practices in maintaining stocks of SOC. We describe here a simple model of SOC turnover at the soil profile scale that accounts for two key processes determining SOC persistence (i.e. microbial energy limitation and physical protection due to soil aggregation). We tested the model and evaluated the identifiability of key parameters using topsoil SOC contents measured in three treatments with contrasting organic matter inputs (i.e. fallow, mineral fertilized and cropped, with and without straw addition) in a long-term field trial. The estimated total input of organic matter (OM) in the treatment with straw added was roughly three times that of the treatment without straw addition, but only 12% of the additional OM input remained in the soil after 54 years. By taking microbial energy limitation and enhanced physical protection of root residues into account, the model could explain the differences in C persistence among the three treatments, whilst also accurately matching the time-courses of SOC contents using the same set of model parameters. Models that do not explicitly consider microbial energy limitation and physical protection would need to adjust their parameter values (either decomposition rate constants or the retention coefficient) to match this data.

We also performed a sensitivity analysis to identify the most influential parameters in the model determining soil profile stocks of OM at steady-state. Input distributions for soil and crop parameters in the model were defined for the agricultural production area of PO4 (east-central Sweden), which includes Uppsala. This analysis showed that model parameters affecting SOC decomposition rates, including the rate constant for microbial-processed SOC and the parameters regulating physical protection and microbial energy limitation, are more sensitive than parameters determining OM inputs. The development of pedotransfer approaches to estimate SOC decomposition rates from soil properties would therefore support predictive applications of the model at larger spatial scales.

1   Introduction

Adopting soil and crop management practices that increase stocks of soil organic carbon (SOC) is one promising way to mitigate climate change, whilst simultaneously improving soil health (Paustian et al., 2016; Baveye et al., 2020). In conjunction with long-term field experiments, simulation models are useful tools for testing our understanding of the processes involved in the turnover of SOC and for evaluating the potential of management practices to enhance SOC sequestration. Most model applications to date have focused on cultivated topsoil, which is clearly of major importance with respect to the effects of soil management on SOC and soil health. However, subsoils contain a large proportion of the total stock of SOC (Batjes, 1996; Jobbágy and Jackson, 2000; Poeplau et al., 2020) and residence times are also much longer (Rumpel and Kögel-Knabner, 2011; Sierra et al., 2024; Button et al., 2022). This may indicate a significant potential for long-term C sequestration of root-derived OM in subsoils, which could be of substantial benefit in mitigating climate change.

Several detailed mechanistic models have been developed that describe a wide range of processes affecting C stocks at the scale of the entire soil profile, including soil water flow, transport of dissolved organic carbon by advection-diffusion and bioturbation, as well as descriptions of SOC decomposition explicitly accounting for microbial processes (e.g. Izaurralde et al., 2006; Braakhekke et al., 2011; Riley et al., 2014; Ahrens et al., 2015; Camino-Serrano et al., 2018; Hicks Pries et al., 2018; Keyvanshokouhi et al., 2019; Yu et al., 2020). Such mechanistic models are useful tools for improving process understanding (Smith et al., 2018; Derrien et al., 2023), but parameter uncertainty and the ever-present likelihood of equifinality means that predictive model applications may be problematic (Braakhekke et al., 2013). Simpler empirical (phenomenological) models of SOC turnover and storage may have an advantage in this respect because they require fewer parameters (Derrien et al, 2023).

Although simple models are in principle well suited to policy and management applications, their validation status is generally poor: many have been extensively calibrated against field observations, but their reliability in extrapolation (i.e. prediction of independent data) has not yet been convincingly demonstrated (Garsia et al., 2023; Le Noë et al., 2023). This is because these models have often been tested against limited datasets (i.e. observations of topsoil C dynamics at a single site and treatment) which increases the likelihood of equifinality despite the small number of parameters (e.g. Juston et al., 2010; Luo et al., 2017). This may be overcome by simultaneous calibration of the model against data for two or more contrasting treatments, for example with respect to the type and quantity of organic matter inputs (e.g. Meurer et al., 2020) or by multi-site calibration at larger scales using data from long-term field trials at locations with contrasting soils and management practices (e.g. Juston et al., 2010; Dechow et al., 2019). Testing model predictions for entire soil profiles remains however difficult and is therefore rarely done, because fewer measurements are made in subsoils and the turnover of organic C in subsoil is very slow, so datasets will rarely be long enough to detect any changes. Additional data sources may also help to alleviate problems arising from equifinality. One possibility is to make use of ^{14}C concentrations as a measure of SOC age (e.g. Braakhekke et al., 2014; Ahrens et al., 2015; Sierra et al., 2018) or concentrations of natural stable isotopes of C (Balesdent and Mariotti, 1987), their ratio ^{12}C/^{13}C in C3-C4 vegetation chronosequences (Schiedung et al., 2017) or labelled material (Sanaullah et al., 2011). If such data is missing, an alternative approach to model validation is to compare model predictions against spatial (soil survey) datasets either at catchment, regional or national scales. This has often been done for the topsoil (e.g. Sleutel, et al., 2006; Yagasaki and Shirato, 2014), but to our knowledge there are no examples of this approach in the published literature dealing with total stocks of organic C in the profile.

Ideally, a model that is intended for predictive applications should combine the advantages of simplicity with descriptions that adequately capture or mimic the most important processes determining SOC stocks for the temporal and spatial scales of interest (Campbell and Paustian, 2015). In this respect, the evidence suggests that turnover of SOC is affected mostly by bioavailability (i.e. soil properties controlling adsorption; Mathieu et al., 2015), physical protection (e.g. Killham et al., 1993; Strong et al., 2004; Salomé et al., 2010) and the amount of SOC as it provides energy for microbial biomass growth, maintenance and activity (e.g. Fontaine et al., 2007; Don et al., 2013; Wutzler and Reichstein, 2013). In this study, we describe a simple model that is specifically designed to mimic these key processes at the scale of a soil profile. The model structure is based on ICBM (**I**ntroductory **C**arbon **B**alance **M**odel; Andrén and Kätterer, 1997), which contains two C pools (young particulate and old microbial processed SOC). This simple model based on first-order kinetics was further developed by Meurer et al. (2020) to account for the interactions of soil organic matter (SOM) with soil physical properties to enable

78 simulation of physical protection due to soil aggregation. More recently, Coucheney et al. (2024) further developed

79 the model to account for the effects of SOC stocks on decomposition rates due to microbial energy limitation (i.e.

80 positive and negative priming) following an approach originally proposed by Wutzler and Reichstein (2013).

81 Compared with the original ICBM model (Andrén and Kätterer, 1997), this new model only requires two additional

82 parameters, one to account for physical protection and one for microbial energy limitation. It is therefore still

83 relatively simple, neglecting several potentially important processes affecting SOC stocks in the soil profile,

84 particularly transport processes such as the advection and diffusion of dissolved organic C as well as bioturbation.

85 However, using a more complex process-oriented model, Sierra et al. (2024) recently concluded that these

86 transport processes are generally only of limited importance for subsoil SOC stocks, which are instead largely

87 determined by the balance between root-derived inputs and decomposition rates.

88 Coucheney et al. (2024) introduced this simple model of SOC turnover into the new soil-crop model USSF

89 (**U**ppsala model of **S**oil **S**tructure and **F**unction; Jarvis et al., 2024) and used it to evaluate the potential of winter

90 wheat ideotypes with improved root system characteristics to enhance SOC stocks in a structured clay soil in

91 Uppsala. In doing so, Coucheney et al. (2024) parameterized the SOC model from literature information, as the

92 available site data was thought to be insufficient to unequivocally identify the model parameters. In this paper, we

93 describe the SOC model and present a test of model predictions and parameter identifiability using organic C

94 concentrations measured in the topsoil of three treatments with strongly contrasting OM inputs in a long-term field

95 experiment in Uppsala. We also perform a Monte Carlo sensitivity analysis to identify the most influential

96 parameters in the model determining estimates of total stocks of SOC in the soil profile at steady-state. Input

97 distributions for soil and crop parameters were defined for the agricultural production area (PO4) in east-central

98 Sweden that encompasses Uppsala. Geo-referenced data that would enable a spatially explicit test of the model for

99 this region was not available. Instead, aggregated regional-scale soil survey data was used as a qualitative "reality-

100 check", assuming that profiles of SOC are approximately at steady-state. The overall aim of this study is to

101 demonstrate the utility of a simple soil C turnover model that can account for the nexus of soil management, soil

102 structure and microbial activity that critically determines C mineralization and stabilization at the scale of a soil

103 profile.

104 ## 2   Materials and Methods

105 In the following, we first describe a new parsimonious model of OM turnover applicable to a single topsoil horizon,

106 which we test using data from three contrasting cropping and fertilization treatments in the Ultuna Long-Term Soil

107 Organic Matter Experiment. We then derive a steady-state solution of the model and also show how it can be

108 extended to describe OM storage and turnover in a complete soil profile. Finally, these profile-scale steady-state

109 solutions are used to support a regional-scale sensitivity analysis and reality-check.

110 ### 2.1   Model description

111 #### 2.1.1   SOM turnover and storage in a single soil horizon

112 A dual-porosity model describing the two-way interactions between soil physical properties and SOM stocks and

113 turnover was described by Meurer et al. (2020). In this model, SOM contents influence the total porosity and its

114 partitioning between two pore regions in the soil (i.e. mesopores and micropores) using a simple model that

115 describes how SOM affects aggregation. In turn, the pore size distribution determines the partitioning of root-

116 derived inputs of OM between the two pore regions. This means that compared with a sandy soil, a larger

proportion of the root OM input will enter the micropore region in a clay soil, as it predominantly consists of smaller pores. The soil pore size distribution also regulates decomposition rates with slower decomposition rates of OM stored in microporous regions of the soil. Compared with sandy soils, clay soils therefore have a greater potential for physical protection of soil C. Coucheney et al. (2024) introduced a description of the effects of microbial energy limitation according to the "*LimUptake*" variant of the model suite described by Wutzler and Reichstein (2013) into the SOM model described by Meurer et al. (2020). They also simplified the description of the transfer of SOM between the two pore regions by tillage, making the assumption that there is always a net transfer of SOM from micropore to mesopore regions. This should give more realistic simulations of the effects of tillage on SOM and also has the added benefit of allowing a straightforward solution of the model for steady-state conditions.
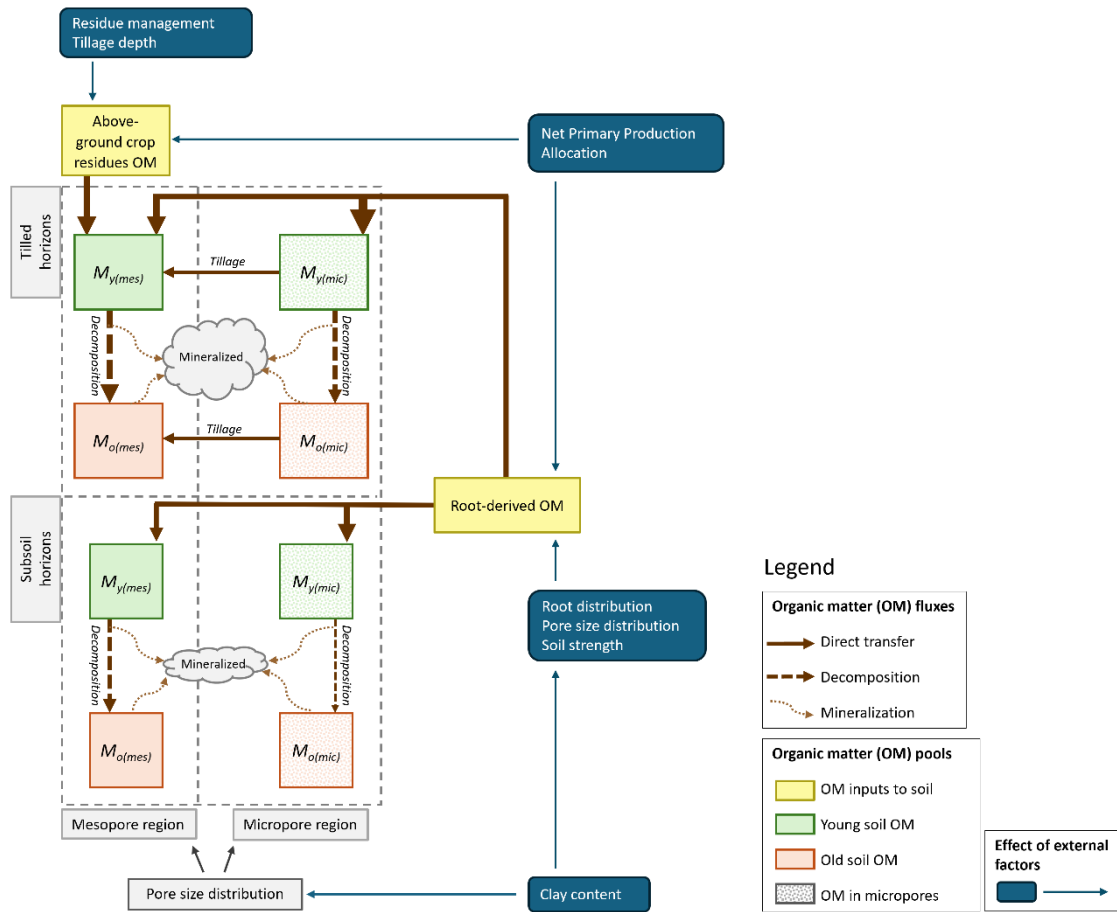
Figure 1. Schematic diagram of the organic matter (OM) pools and fluxes and of the main external factors affecting OM inputs to the soil (for definitions see equations 1 to 6, 10 to 13 and 20 to 24). The grey boxes with dashed lines indicate tilled and subsoil horizons in the soil profile, both partitioned between two pore regions (micropores and mesopores). This partitioning is estimated from the soil clay content using pedotransfer functions (equations 10 to 13). OM located in the micropores is partially physically protected from decomposition (by a factor F_p see equations 3 and 4). In tilled horizons, OM from the above-ground crop residues is added only to the mesopore region and a fraction of OM located in the micropores is transferred by tillage. Root-derived OM is added to both pore regions as a function of pore size distribution and soil strength through effects on root distribution in the soil profile (see equations 21-24). The sizes of the boxes and arrows illustrate that OM contents and fluxes are generally smaller in subsoil as a result of lower OM inputs, which, in turn, leads to greater energy limitation (equations 5 and 6).

128 The model tracks four pools of SOM, two pools of young OM ($M_{Y(mic)}$ and $M_{Y(mes)}$) and two pools of older

129 microbial-processed SOM ($M_{O(mic)}$ and $M_{O(mes)}$) (see Fig. 1). For both types, one part is stored in microporous

130 regions of the soil (subscript "mic") where it is partially protected from decomposition, while the remainder is

131 stored in regions of the soil in contact with larger mesopores (subscript "mes"), which facilitates faster

132 decomposition (see Fig. 1). Changes in the mass of SOM in the four pools (kg m^{-2}) in a horizon are given by:

133
$$\frac{dM_{Y(mes)}}{dt} = I_a + I_r\left(1 - f_{r,mic}\right) - k_Y k_{u(mes)} M_{Y(mes)} + k_{till} M_{Y(mic)} \tag{1}$$

134
$$\frac{dM_{O(mes)}}{dt} = \left(\varepsilon\, k_Y k_{u(mes)} M_{Y(mes)}\right) - \left((1-\varepsilon)\, k_O k_{u(mes)} M_{O(mes)}\right) + k_{till} M_{O(mic)} \tag{2}$$

135
$$\frac{dM_{Y(mic)}}{dt} = I_r f_{r,mic} - k_Y k_{u(mic)} F_p M_{Y(mic)} - k_{till} M_{Y(mic)} \tag{3}$$

136
$$\frac{dM_{O(mic)}}{dt} = \left(\varepsilon\, k_Y k_{u(mic)} F_p M_{Y(mic)}\right) - \left((1-\varepsilon)\, k_O k_{u(mic)} F_p M_{O(mic)}\right) - k_{till} M_{O(mic)} \tag{4}$$

137 where I_a and I_r (kg m^{-2} yr^{-1}) are the supply of OM from above-ground residues and roots respectively, $f_{r,mic}$ (-) is

138 the proportion of the root-derived OM added to the micropore region, ε (-) is the SOM retention coefficient, k_Y and

139 k_O (yr^{-1}) are reference rate constants for the decomposition of young and old SOM. k_{till} (yr^{-1}) is a rate constant

140 regulating the transfer of SOM between pore regions by tillage, F_p (-) is a factor varying from zero to unity that

141 reduces OM decomposition rates in the micropore region to account for physical protection and $k_{u(mes)}$ and $k_{u(mic)}$

142 (-) are microbial energy limitation factors given by the simple model described by Wutzler and Reichstein (2013):

143
$$k_{u(mes)} = max\left\{0; \left(1 - \frac{A_a}{\varepsilon\left(k_Y\left(\frac{M_{Y(mes)}}{\Delta z}\right) + k_o\left(\frac{M_{o(mes)}}{\Delta z}\right)\right)}\right)\right\} \tag{5}$$

144
$$k_{u(mic)} = max\left\{0; \left(1 - \frac{A_a}{\varepsilon F_p\left(k_Y\left(\frac{M_{Y(mic)}}{\Delta z}\right) + k_o\left(\frac{M_{o(mic)}}{\Delta z}\right)\right)}\right)\right\} \tag{6}$$

145 where A_a (kg m^{-3} yr^{-1}) is a composite microbial parameter that represents a minimum C uptake flux that can support

146 an active microbial biomass and Δz is the horizon thickness (m).

147 Soil bulk density, γ_b (kg m^{-3}) and OM content f_{som} (kg kg^{-1}) are calculated from the stocks of OM as inter-linked

148 variables (Meurer et al., 2020):

149
$$\gamma_b = \frac{M_{tot} + \left(\Delta z_{min}\gamma_m(1 - \phi_{min})\right)}{\Delta z} \tag{7}$$

150
$$f_{som} = \frac{M_{tot}}{\Delta z\, \gamma_b} \tag{8}$$

151 where M_{tot} (kg m^{-2}) is the total OM stock ($= M_{Y(mes)} + M_{O(mes)} + M_{Y(mic)} + M_{O(mic)}$), γ_m (kg m^{-3}) is the density of mineral

152 matter in soil and ϕ_{min} is the textural porosity in soil (m^3 m^{-3}). The horizon thickness in equations 5 to 8 varies due

153 to soil aggregation (Meurer et al., 2020):

154
$$\Delta z = \Delta z_{min} + \left\{\left(1 + f_{agg}\right)\left(\frac{M_{tot}}{\gamma_o}\right)\right\} \tag{9}$$

155 where f_{agg} (m^3 m^{-3}) is the aggregation factor, γ_o (kg m^{-3}) is the density of SOM and Δz_{min} (m) is the minimum layer

156 thickness in a soil without SOM and aggregation porosity.

157 Meurer et al. (2020) equated $f_{r,mic}$ in equations 1 and 3 with the micropore fraction of the soil pore space, which

158 varied with changes in OM stocks in each pore region. Here, in order to derive a solution for OM stocks at steady-

159 state (see "Steady-state solution for SOM stocks"), the fraction of the root-derived OM added to the micropore

160 region ($f_{r,mic}$ in equations 1 and 3) is assumed to be a constant and is calculated from a micropore fraction of the

161 pore space f_{mic} (-) estimated from the soil clay content, weighted by a dimensionless constant w ($0 \leq w \leq 1$) to

162 account for the effects of soil strength on the distribution of roots between the two pore regions. Using a power

163 law function for the pore size distribution gives:

164 $$f_{r,mic} = w\, f_{mic} = w \left(\frac{\psi_{ae}}{\psi_{mic}} \right)^{\lambda} \qquad (10)$$

165 where ψ_{ae} and ψ_{mic} are the air-entry pressure head (m) and the pressure head (m) equivalent to the largest micropore

166 in the soil respectively and λ (-) is the pore size distribution index (Brooks and Corey, 1964), which is here

167 estimated from soil clay content f_{clay} (kg kg^{-1}) using the pedotransfer functions for field capacity θ_{fc} and wilting

168 point θ_w (m^3 m^{-3}) derived from a database of water retention curves for Swedish agricultural soils by Kätterer et

169 al. (2006):

170 $$\lambda = \frac{\log\left(\frac{\theta_w}{\theta_{fc}}\right)}{\log\left(\frac{0.5}{150}\right)} \qquad (11)$$

171 $$\theta_{fc} = 0.27 + 0.325\, f_{clay} \qquad (12)$$

172 $$\theta_w = 0.004 + 0.5 f_{clay} \qquad (13)$$

173 Thus, in this simpler version of the model described by Meurer et al. (2020), changes in SOM contents affect the

174 porosity and bulk density but not the pore size distribution.

175 **2.1.2 Steady-state solution for SOM stocks**

176 From equations 1 to 4, steady-state SOM stocks in the four pools are given as:

177 $$M_{Y(mic)} = \left(\frac{I_r f_{r,mic}}{\{k_Y F_p k_{u,mic}\} + k_{till}} \right) \qquad (14)$$

178 $$M_{Y(mes)} = \left(\frac{I_a + I_r(1 - f_{r,mic}) + \{k_{till} M_{Y(mic)}\}}{k_Y k_{u,mes}} \right) \qquad (15)$$

179 $$M_{O(mic)} = \left(\frac{\varepsilon k_Y k_{u,mic} F_p M_{Y(mic)}}{\{(1-\varepsilon) k_O F_p k_{u,mic}\} + k_{till}} \right) \qquad (16)$$

180 $$M_{O(mes)} = \left(\frac{\{\varepsilon k_Y k_{u,mes} M_{Y(mes)}\} + k_{till} M_{O,mic}}{(1-\varepsilon) k_O k_{u,mes}} \right) \qquad (17)$$

181 Equations 14 to 17 show that the steady-state stocks depend on k_u, while k_u, in turn, depends on the stocks

182 (equations 5 and 6). An iterative procedure is first used to derive a value of $k_{u(mic)}$ at steady-state that simultaneously

183 satisfies equations 6, 14 and 16. The steady-state stocks in the mesopore region (equations 15 and 17) depend on

184 the value of $k_{u,mes}$ at steady-state. This can now be calculated directly by substituting equations 15 and 17 into

185 equation 5:

186 $$k_{u,mes} = \cfrac{1}{1 + \left\{ \cfrac{A_a\,\Delta z}{\varepsilon\left(i^* + \left(\frac{\varepsilon i^* + k_{till}M_{O(mic)}}{1-\varepsilon}\right)\right)} \right\}}$$ (18)

187 where i^* is the input of OM to the mesopore region given by:

188 $$i^* = I_a + I_r\left(1 - f_{r,mic}\right) + k_{till}M_{Y(mic)}$$ (19)

2.1.3 Application of the model to a soil profile

190 The model can be applied to a soil profile consisting of two or more soil horizons by expressing k_{till}, I_a, I_r, and w

191 as a function of soil depth, keeping all the other parameters constant. For the sake of simplicity, the textural porosity

192 ϕ_{min} (equation 7) could also vary with depth in the soil, but it is assumed to take a constant value in the following,.

193 Tillage is here assumed to affect SOM turnover only in the uppermost horizon, with k_{till} set to zero for all other

194 horizons. Above-ground crop residues I_a are given by:

195 $$I_a = Y\left(\frac{1}{HI} - 1\right)f_{inc}$$ (20)

196 where Y is the yield (kg m^{-2}), HI (-) is the harvest index (the ratio of yield to total above-ground biomass) and f_{inc}

197 is the proportion of the above-ground residues incorporated into soil. The partitioning of I_a among the soil horizons

198 can be defined by the user, but should reflect tillage systems and depths of cultivation. The total input of root-

199 derived OM, I_r is given by:

200 $$I_{r(tot)} = \frac{Y\,f_{bg}}{HI(1 - f_{bg})}$$ (21)

201 where f_{bg} is the proportion of net primary production that is allocated below-ground, including both root growth

202 and exudates. Root-derived OM is added to the soil horizons in the profile according to a two-parameter logistic

203 function, which represents the distribution of roots with depth in the soil (e.g. Schenk and Jackson, 2002; Fan et

204 al., 2016):

205 $$P = \frac{1}{1 + \left(\frac{z}{D_{50}}\right)^c}$$ (22)

206 where P is the fraction of the total root biomass found above a depth z, representing the lower boundary of the

207 horizon in question, c is a root distribution parameter and D_{50} is the depth above which 50% of the root biomass

208 is recovered, which is given by:

209 $$D_{50} = \frac{D_{95}}{\left(\frac{1}{0.95} - 1\right)^{\frac{1}{c}}}$$ (23)

210 where D_{95} is the depth (m) above which 95% of the total root biomass is recovered. With this function, a small

211 fraction of the root biomass is found below the depth of the soil profile. This additional fraction of the root biomass

212 is added to the upper two horizons in equal amounts.

213 Finally, the weighting function to account for the effects of soil strength on the distribution of roots between the

214 two pore regions is given by:

215 $$w = EXP\left(-w_s(z - z_1)\right)$$ (24)

where the constant w_s (m^{-1}) reflects the effects of increasing soil strength with depth on the distribution of roots between soil micropore and mesopore regions and z_1 is the depth to the lower boundary of the uppermost soil horizon. It can be seen from equation 24 that $w = 1$ for the uppermost horizon, so that the root-derived OM in this layer is partitioned between the pore regions directly proportional to their estimated respective partial volumes.

Figure 2. Map of Sweden (in white) showing the location of the Ultuna Long-term Soil Organic Matter Experiment (Uppsala, Sweden) and the extent of the production area PO4 (shaded area in grey). Drawn by Anna Lindahl, SLU, from Esri, TomTom, Garmin, FAO, NOAA, and USGS

2.2   Model applications

2.2.1   Long-term transient simulations of SOC under contrasting cropping and fertilization

We performed a test of the model described by equations 1 to 13 using data from the Ultuna Long-Term Soil Organic Matter Experiment located at Uppsala, east-central Sweden (59.8° N, 17.7° E; Fig. 2; Pold et al., 2025). The mean annual temperature at Ultuna is 7 °C and the mean annual precipitation is 570 mm. The texture in the uppermost 20 cm of soil is clay loam (37 % clay, 41 % silt and 22 % sand). In this study, we make use of SOC contents measured in the topsoil (0-20 cm depth) from the start of the trial in 1956 until 2010 in three treatments with contrasting inputs of organic matter: an uncropped fallow treatment (*"Fallow"*) and two cropped treatments

("N fertilized" and "N fertilized + straw"), both of which are supplied with $Ca(NO_3)_2$ every year at the time of sowing at a rate of 80 kg N ha^{-1} year^{-1}. Most (ca. 95%) of the above-ground crop residues are removed at harvest in autumn and straw is applied biennially to the treatment "N fertilized + straw" after harvest at an equivalent annual rate of 4.2 t ha^{-1}. Maize (*Zea mays*) has been grown on the cropped plots since 2000. Before 2000, the crop rotation included barley (*Hordeum vulgare*), oats (*Avena sativa*), beets (*Beta vulgaris*) (prior to 1967) and rape (*Brassica napus*). All the plots are dug by hand after harvest each year to a depth of 20 cm to simulate ploughing as the plots are too small (4 m^2) to be managed in the same way as a farmer's field. We refer readers to Persson and Kirchmann (1994) and Kätterer et al. (2011) for more details of the design of the field experiment.

Inputs of OM from above-ground crop residues and root-derived OM were estimated following Kätterer et al. (2011), who made use of the allocation functions dependent on crop yields derived by Bolinder et al. (2007), together with a Michaelis-Menten function to estimate the proportion of the root-derived OM that was presumed to have been input to the topsoil (0-20 cm). Here, we simplified this method by using average OM inputs in each treatment for the experimental period (1956-2010) based on annual values calculated for the different crops in the rotation.

The model was simultaneously calibrated to the measurements of total SOC from the three treatments using the Generalized Likelihood Uncertainty Estimation (GLUE) method (Beven, 2006; Beven and Binley 2014; Juston et al., 2010). This is because we wanted to critically test the model to see if it was possible to obtain acceptable parameterizations common to all three of the treatments. Inspection of the model equations led us to expect to encounter significant equifinality. Therefore, only six of the fifteen parameters were included in the GLUE analysis, with their prior uncertainty ranges shown in Table 1. The OM supply prior to the start of the experiment and the fraction of this OM supplied as straw, were included in the calibration process to help initialize the SOM pools during a common 5000-year spin-up period. Four remaining parameters, which were considered difficult to identify "a priori" from experimentation, but which were expected to be sensitive and therefore potentially identifiable by calibration, were treated as uncertain (Table 1). We ran 12000 simulations using Latin Hypercube Sampling to sample uniform distributions between the minimum and maximum values for the six uncertain parameters (Table 1). The remaining nine parameters were set to fixed values (Table 2) as they could be estimated from measurements (e.g. f_{clay}, f_{agg}, F_p) or they were not expected to be sensitive (e.g. k_y, Andrén and Kätterer, 1997; Juston et al., 2010; Meurer et al., 2020), or both (e.g. ψ_{ae}, ψ_{mic}, ϕ_{min}, γ_o, γ_m). These fixed parameters included the soil physical properties, since an analysis of soil structure dynamics was not the main focus of this modelling study, which employs a slightly simplified description of the interactions between soil aggregation and SOM. It can be noted that the final bulk densities for the 30 best simulations (see below) derived varied between 1.2 and 1.3 g cm^{-3} using the fixed parameter values shown in Table 2 (with "N fertilized + straw" < "N fertilized" < "Fallow"). This matched reasonably well the magnitude and order of the measured values reported for the three treatments in Kätterer et al. (2011), which were 1.43, 1.28 and 1.21 g cm^{-3} respectively.

266 **Table 1. Six model parameters selected for the calibration to the Ultuna Long-Term Soil Organic Matter**
267 **Experiment and their initial parameter uncertainty ranges**

Parameter	Symbol	Units	Prior uncertainty ranges
Total OM input during spin-up	$I_a + I_r$	kg m^{-2} y^{-1}	0.25-0.45
Straw fraction of OM input during spin-up	$I_a/(I_a + I_r)$	-	0.65-0.85
Rate constant for OM transfer by tillage between pore regions	k_{till}	y^{-1}	0.00- 0.01
Reference decomposition rate constant for old OM	k_o	y^{-1}	0.06- 0.10
OM retention coefficient	ε	-	0.20- 0.45
Microbial energy limitation factor	A_a	kg m^{-3} y^{-1}	0.10- 0.30

268 **Table 2. Nine model parameters fixed at constant values during the calibration based on field**
269 **measurements at Ultuna or literature data**

Parameter	Symbol	Units	Value	Source
Clay content	f_{clay}	kg kg^{-1}	0.36	Persson and Kirchmann (1994); Pold et al. (2025)
Density of organic matter	γ_o	kg m^{-3}	1200	Meurer et al. (2020); Coucheney et al. (2024)
Density of mineral matter	γ_m	kg m^{-3}	2700	Meurer et al. (2020); Coucheney et al. (2024)
Textural porosity	ϕ_{min}	m^3 m^{-3}	0.5	Coucheney et al. (2024)
Aggregation factor	f_{agg}	m^3 m^{-3}	3	Meurer et al. (2020)
Physical protection factor	F_p	-	0.2	Kravchenko et al. (2015)
Air-entry pressure head	ψ_{ae}	m	0.2	Coucheney et al. (2024)
Pressure head equivalent to the largest micropore in soil	ψ_{mic}	m	6.0	Killham et al. (1993); Strong et al. (2004); Ruamps et al. (2011)
Reference decomposition rate constant for young OM	k_y	y^{-1}	0.8	Andrén and Kätterer (1997)

270 The model efficiency *EF* was used as the likelihood function in GLUE:

271 $$EF = 1 - \frac{\sum_{i=1}^{n}(O_i - P_i)^2}{\sum_{i=1}^{n}(O_i - \bar{O})^2} \qquad (25)$$

272 where O and P are observed and predicted values, $\bar{O}$ is the mean of the observations and n is the number of

273 observations. The maximum value of *EF* is one, when predictions and observations are identical, while a negative

274 value implies a poor model, since it means that taking the average of the observations would give a better

275 prediction. For each simulation, individual model efficiencies were calculated for each treatment and the mean EF

276 value for the three treatments was used as a metric to identify acceptable parameters sets. This was done to obtain

277 a robust parameterization by selecting parameter sets that simultaneously fitted all three treatments well. The

278 number of acceptable parameter sets was determined such that the range of variation of their predictions
279 approximately covered the variations observed in the measurements. With this criterion, 30 of the 12000
280 parameter sets were identified as acceptable. Note that this low acceptance rate is a consequence of the
281 inefficient sampling inherent to the GLUE method and says nothing about the quality of the model.

282 **2.2.2   Steady-state calculations: sensitivity analysis and reality-check**
283 We performed a Monte Carlo sensitivity and uncertainty analysis to assess the relative importance of 15 model
284 parameters for predictions of the steady-state stocks of SOM in the soil profile (equations 7 to 24; Table 3). The
285 analysis was based, to the extent possible, on data and information available for the Ultuna field site as well as soil
286 survey and cropping data (e.g. crop yields, soil clay content) for the agricultural production area PO4 in east-
287 central Sweden (i.e. the region in which Ultuna is located; Fig. 2). Literature information was used to determine
288 parameter distributions in the absence of data at the local or regional scale (Table 3). We assumed normal
289 distributions when the data was considered sufficient to support such a distribution. Uniform distributions were
290 used otherwise (Table 3). One thousand parameter sets were generated from these distributions by random
291 sampling.

292 Calculations were performed for a soil profile 120 cm in depth, divided into four soil horizons (0-20, 20-40, 40-
293 60 and 60-120 cm). We added 80% of the above-ground residues I_a (equation 20) to the uppermost horizon in the
294 soil profile and the remaining 20% to the horizon below. For all 1000 parameter sets, we calculated the SOM stock
295 in each horizon and in the whole soil profile at steady-state. For each soil horizon, we also calculated the steady-
296 state bulk density and SOM contents as well as the mean residence time of SOM as the steady-state SOM stock
297 divided by the input/output flux.

298 We used a multiple linear regression model to characterize variations in the steady-state SOM stocks in the profile
299 (y), such that the normalized coefficients (β_1, β_2 ... β_n) can be used as a metric of sensitivity to variation in the
300 parameters (x_1, x_2 ... x_n) (Saltelli and Annoni, 2010):

301 $$y = \beta_0 + \beta_1 x_1 + \beta_2 x_2 + \ ....\beta_n x_n \tag{26}$$

302 Aggregated data for SOC contents measured at three depth intervals (0-20, 20-40 and 40-60 cm depth) for soils in
303 production area PO4 (n = 611, 100 and 100 respectively) were extracted from the national soil and crop inventory
304 carried out from 2001 to 2007 (Eriksson et al., 2010) and used as a qualitative "reality-check" for the model
305 calculations. Note that, as a consequence of simulating links to soil physical properties, the model calculates SOM
306 contents, whereas SOC was measured. In converting from one to the other, we assumed that organic C constituted
307 50% of the SOM. Likewise, calculated bulk densities at zero to 20 cm and 40 to 60 cm depth were compared with
308 data available for soil profiles (n = 54) located in the production area PO4 (Klöffel et al., 2024). The model
309 parameters required to convert calculated SOM stocks to estimates of SOM contents using equations 7 to 9 were
310 set to the fixed values used in the model calibration (Table 2), with the exception of the textural porosity which
311 was reduced from 0.5 to 0.4, as the latter value was considered to be more representative for most soils (Klöffel et
312 al., 2024). Note that the textural porosity was also assumed to be constant with depth in the soil.

313

Table 3. Parameter input distributions in the sensitivity analysis. In the case of uniform distributions, minimal and maximal values are shown (Min.; Max.) while in the case of normal distribution the mean and standard deviation are shown (Mean; St. dev.).

Group	Parameters (symbol, unit)	Distribution	Source
Crop growth and residue inputs	Yield (Y, kg m^{-2})	Normal (0.50; 0.05)	SCB, Statistics Sweden: https://www.statistikdatabasen.scb.se/pxweb/en/ssd/START__JO__JO0601/SkordarL2/
	Harvest index (HI, -)	Normal (0.40; 0.05)	Hay (1995); Kätterer et al. (1997); Coucheney et al. (2024)
	Fraction of net primary production allocated belowground (f_{bg}, -)	Normal (0.200; 0.025)	Bolinder et al. (2007); Kätterer et al. (2011)
	Fraction of aboveground crop residues incorporated (f_{inc}, -)	Normal (0.65; 0.10)	Smerald et al. (2023)
	Root depth (D_{95}, m)	Uniform (0.8; 1.2)	Jackson et al. (1996); Kätterer et al. (2011); Fan et al. (2016)
	Root distribution factor (c, -)	Uniform (-1.2; -0.9)	Fan et al. (2016)
Tillage	Rate constant for OM transfer between pore regions (k_{till}, y^{-1})	Uniform (0.000; 0.006)	This study
Organic matter turnover	Reference decomposition rate constant for young organic matter (k_Y, y^{-1})	Uniform (0.6; 1.0)	Andrén and Kätterer (1997)
	Reference decomposition rate constant for old organic matter (k_O, y^{-1})	Uniform (0.06; 0.10)	This study
	OM retention coefficient (ε, -)	Uniform (0.30; 0.35)	This study
	Physical protection factor (F_p, -)	Uniform (0.1; 0.3)	Kravchenko et al. (2015)
	Microbial energy limitation factor (A_a, kg m^{-3} y^{-1})	Uniform (0.1; 0.3)	This study
Soil physical properties	Clay content (f_{clay}, kg kg^{-1})	Normal (0.3; 0.1)	Eriksson et al. (2010)
	Factor for soil strength effects on root distribution between pore regions (w_s, m^{-1})	Uniform (2; 4)	This study
	Pressure head defining the largest micropore (ψ_{mic}, m)	Uniform (-30; -6)	Killham et al. (1993); Strong et al. (2004); Ruamps et al. (2011)

314

3   Results and Discussion

3.1   Long-term transient simulations

Figure 3 shows that the model could be calibrated to match simultaneously the changes in SOC contents measured in the three treatments at the Ultuna Long-Term Soil Organic Matter Experiment during the 50 year period, with the spread of the simulations from the 30 best parameter sets approximately matching the observed variation in SOC among the four replicate plots. Table 4 shows simulated SOM balances for the three treatments. The total input of crop residues in the "N fertilized + straw" treatment is roughly three times that of the "N-fertilized" treatment without straw addition. The calculated inputs of OM derived from roots were similar (Table 4), so that larger inputs of straw accounted for almost all of the difference in OM inputs between these two treatments. However, according to the simulations, almost 88% of the additional OM input in the "N fertilized + straw" treatment was lost as a consequence of enhanced mineralization, with only 12% remaining in the soil. While above-ground crop residues are thought to be less persistent in soil than root-derived residues, the relative importance of several potential underlying mechanisms that could explain this finding is still unclear (e.g. Rasse et al., 2005; Kätterer et al., 2011). It can be noted here that the model does not consider any differences in the quality of root- and straw-derived OM. Instead, the model suggests that the comparatively small difference in OM stocks at the end of the experiment in the two treatments in relation to the large difference in OM inputs is a result of two processes: firstly, straw incorporated in the "N fertilized + straw" treatment is solely added to the mesopore region, which does not afford any physical protection. In contrast, a certain proportion, f_{mic}, of root-derived OM is added to the physically-protected micropore region. Secondly, mineralization rates in the "N-fertilized" treatment without straw addition are reduced by microbial energy limitation as a consequence of an overall decrease in OM stocks due to the near total removal of above-ground crop residues. Taking both these processes into account (physical protection and microbial energy limitation; see equations 1 to 6) enabled the model to reproduce the time-courses of SOC contents in the two treatments with identical parameterizations. Models that do not consider these processes would need to adjust their parameter values (either decomposition rate constants or the retention coefficient) to match this data (e.g. Poeplau et al., 2015).

Figure 4 shows that only one of the parameters included in the calibration procedure (the OM retention coefficient, ε) was well constrained by the data, with acceptable values lying within a narrow range (ca. 0.30 to 0.35). In contrast, for the other five parameters, simulations with large model efficiencies could be found across almost the entire prior uncertainty ranges (Fig. 4). An inspection of the mathematical structure of the model suggests that such a high degree of equifinality should be expected, as many of the key parameters should be strongly correlated (Coucheney et al., 2024). For the 30 best parameter sets, Fig. 5 demonstrates that this is indeed the case for the four parameters regulating decomposition rates in the model (ε, k_o, A_a and k_{till}). These strong correlations of k_o, A_a and k_{till} with ε mean that, in practice, all four parameters are well constrained by the calibration. The acceptable ranges for these four parameters shown in Fig. 5 were utilized in the sensitivity analysis (Table 3).
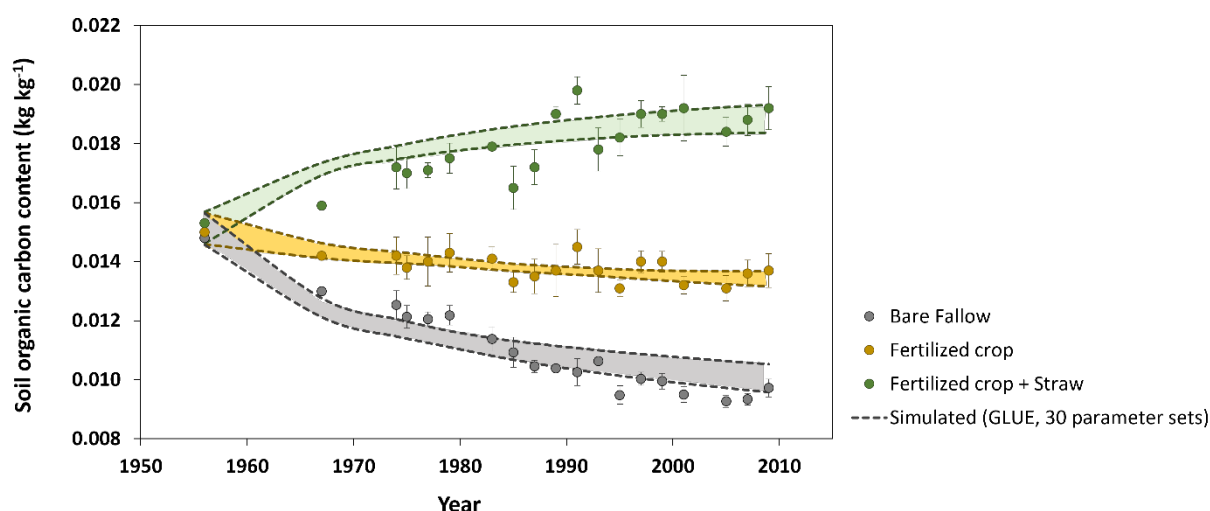
349 **Figure 3. Comparisons of measured SOC contents (symbols are the means of four replicates and the bars**

350 **are standard deviations) with the 30 best simulations from the GLUE analysis (the dashed lines indicate**

351 **ranges)**

352 **Table 4. Simulated mass balances (kg m^{-2}) for SOM for the 55-year experimental period (1956 to 2010) at**

353 **the Ultuna Long-Term Soil Organic Matter Experiment. Values shown for mineralization are the means**

354 **and standard deviations (in brackets) for the 30 best simulations. Values for change of stocks in brackets**

355 **are the percentage changes in relation to the original stock of SOM.**

	Treatment		
Component	Fallow	N fertilized	N fertilized + straw
Inputs:			
- Below-ground residues[1]	0.44	9.85	10.67
- Above-ground residues	0.00	1.82	22.94
- Total crop residue input	0.44	11.67	33.61
Outputs:			
- Mineralization in soil	3.01	12.53	31.75
	(0.18)	(0.16)	(0.20)
Change of SOM stock:	-2.57	-0.86	1.86
	(-35.1%)	(-11.7%)	(+25.4%)

356 [1] estimated using the algorithms presented by Bolinder et al. (2007) and Kätterer et al. (2011)
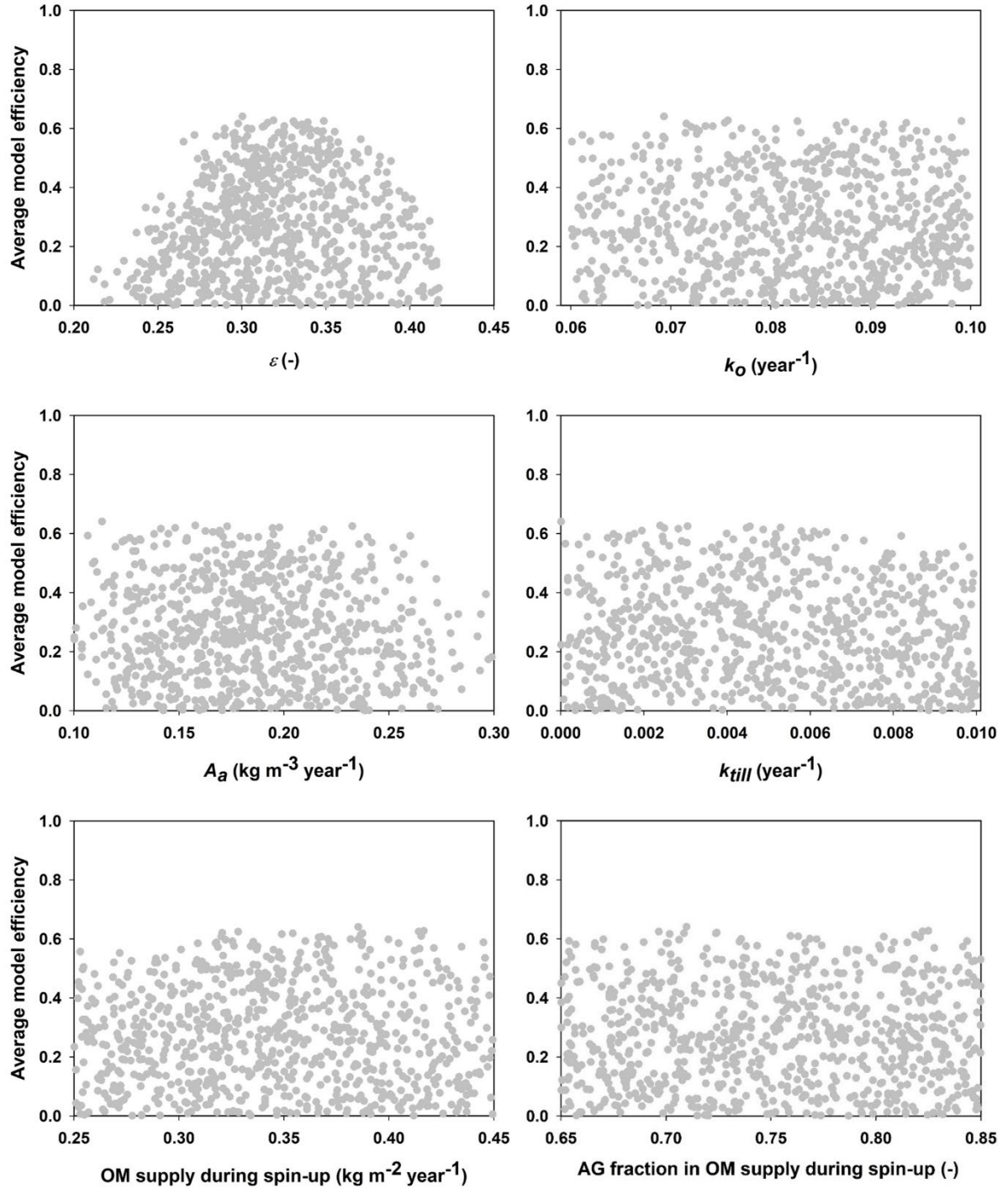
Figure 4. Mean model efficiencies for each parameter set (only simulations with model efficiencies larger than zero are shown) plotted against the values for the six parameters in the GLUE analysis (refer to table 1 for parameter definitions and descriptions; OM = organic matter, AG = above-ground).

3.2   Steady-state calculations

A qualitative comparison with soil survey data for agricultural land in east-central Sweden (production area PO4) suggests that despite its simplicity the model estimates of steady-state SOC and bulk density in the soil profile lie

363 mostly within the range of variation encountered in the region (Fig. 6). Nevertheless, quantile-quantile plots show
364 that the distributions of simulated and measured values of SOC and bulk density are different; especially at the
365 tails, due to the much larger spread in the measurements compared with the calculations and especially the
366 occurrence of a number of outliers with large values of organic carbon contents and small values of bulk density.
367 This is not surprising because the calculations do not include the effects of all factors affecting SOC and bulk
368 density. The large values of SOC content (and small values of bulk density) almost certainly correspond to
369 locations in the PO4 region with wet soils due to topography (i.e. flood plains, depressions). The model, as it is
370 formulated here, does not include the effects of excess soil moisture on decomposition rates. As a further
371 qualitative "reality check", Fig. 7 shows distributions of the mean residence times of SOM calculated for the four
372 horizons in the soil profile. Median values (ca. 20 years) and distributions of residence times estimated for the
373 topsoil are similar to those estimated by Poeplau et al. (2021) for German agricultural soils, and they also lie at the
374 high end of the range in the global analysis reported by Chen et al. (2020) for croplands (mean = 9.5 years, standard
375 deviation = 6 years, n = 217). Taken together with Fig. 6, this gives us confidence that the results of the sensitivity
376 analysis presented in the following should be reasonably well grounded in reality. As also shown by Coucheney
377 et al. (2024), the model simulates much longer mean residence times in subsoil horizons, due to microbial energy
378 limitation and physical protection, with median values of ca. 300 years (Fig. 7).
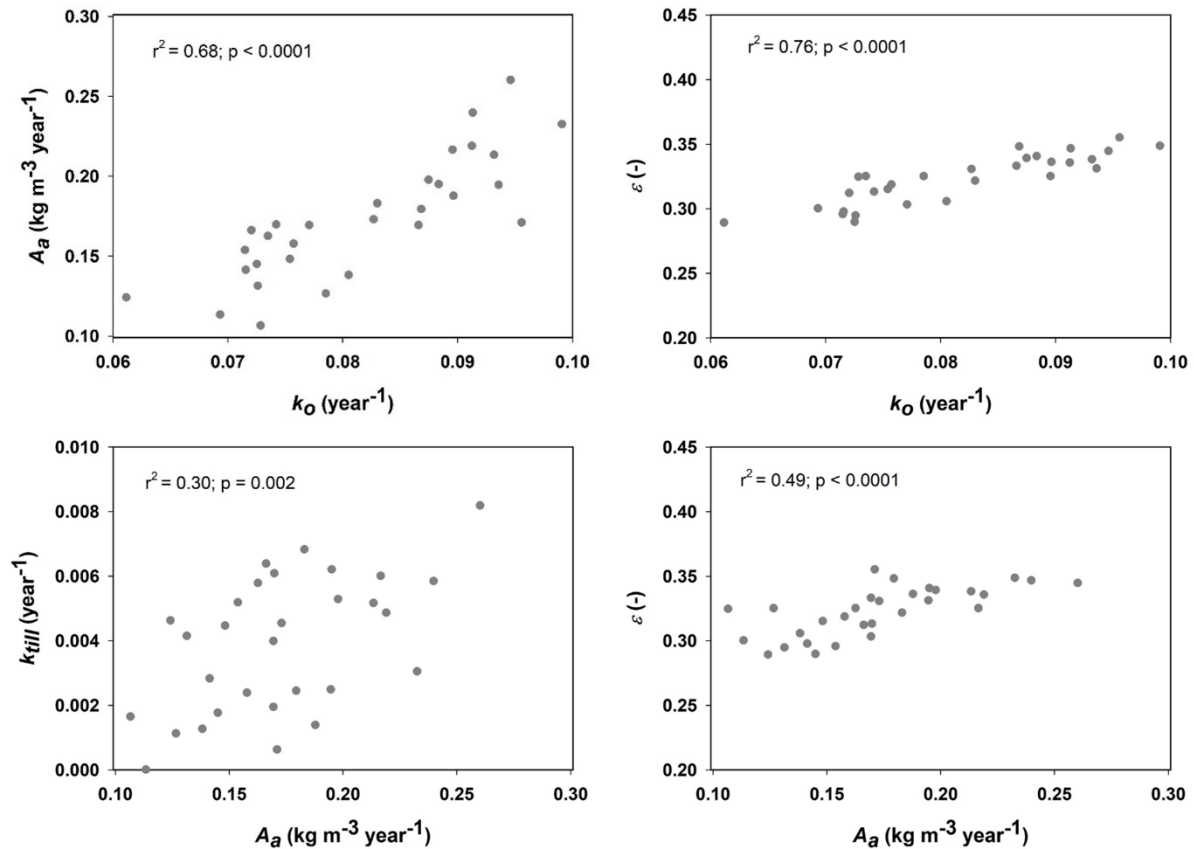
Figure 5. Inter-relationships among four of the six model parameters included in the calibration procedure. Relationships are shown for the 30 best parameter sets identified in the GLUE analysis (refer to table 1 for parameter definitions and descriptions).
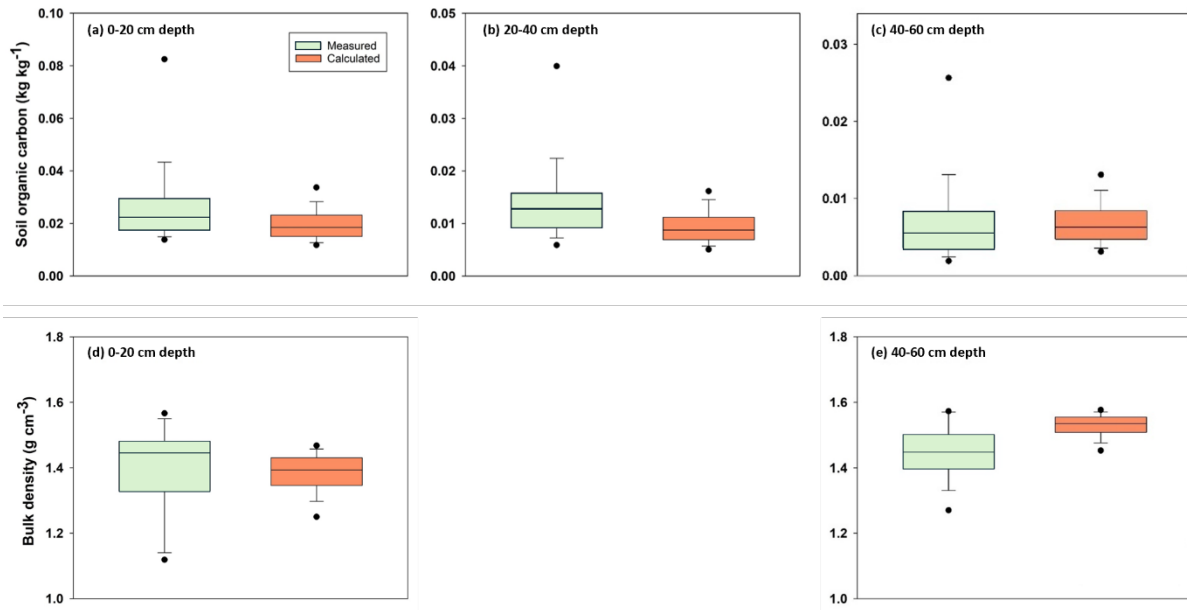
Figure 6. Comparison of the distributions of SOC contents (a to c) and soil bulk density (d and e) measured at three and two depths respectively, for soil profiles located in east-central Sweden (production area PO4; Eriksson et al., 2010) with distributions calculated in the model sensitivity analysis. Horizontal lines show median values, the box defines the inter-quartile range, error bars define 10th and 90th percentiles and solid symbols indicate 5th and 95th percentiles. Note the differences in the y-axis scales for soil organic carbon contents.

Table 5 shows that the most sensitive parameters in the model are those determining decomposition rates of SOM, especially the rate constant for microbial-processed OM, k_o, the parameter regulating microbial energy limitation, A_a, and the parameter regulating the degree of physical protection of OM stored in micropores, F_p. The soil clay content, which together with F_p, determines the extent to which physical protection is expressed in soils of contrasting texture, is also a relatively sensitive model parameter (Table 5). Along with the OM retention coefficient, ε, the three parameters determining inputs of above-ground crop residues (i.e. the fraction incorporated, f_{inc}, and crop yields and harvest index) also exert a strong control on SOM stocks in the soil profile (Table 5). The results of the sensitivity analysis also illustrate the importance of below-ground production for soil profile C stocks calculated by the model (parameter f_{bg}, fraction of NPP allocated below-ground; Table 5), reflecting the assumptions in the model concerning the greater persistence of root-derived OM discussed earlier. An increase of 25% in the fraction of NPP allocated to roots, f_{bg}, increases steady-state SOM stocks by ca. 8%. Transient simulations run with the USSF model for winter wheat grown on Ultuna clay soil presented by Coucheney et al. (2024) illustrate what might be achievable in a shorter 30-year time perspective in the context of climate change mitigation: for the same 25% increase in below-ground C allocation, the USSF model simulated increases in C stocks of ca. 1.4%. In contrast to below-ground production, the sensitivity analysis suggests that root depth and distribution would have little impact on soil profile stocks of OM (Table 5). However, in comparison with soil-crop models such as USSF, the limitations of the simpler model described here should be borne in mind, in particular the lack of any feedback between root system development and crop growth, and thus residue production. In reality, root depth and distribution may play a larger role for soil C stocks. Thus, the transient

404 simulations performed with the full USSF soil-crop model for winter wheat on Ultuna clay soil by Coucheney et
405 al. (2024) suggested that deeper rooting would increase water uptake and crop growth in dry summers, leading to
406 3-5% increases in SOM stocks in a 30-year perspective. Table 5 suggests that tillage is one of the least sensitive
407 factors affecting SOM stocks at steady-state: doubling the tillage intensity parameter in the model, k_{till}, only
408 reduces SOM stocks by 4 to 5%. It must be admitted, however, that the simple description of tillage effects in the
409 model is yet to be rigorously and systematically tested. Nevertheless, in a meta-analysis of long-term experiments
410 in boreal/temperate climates, Haddaway et al. (2017) and Meurer et al. (2018) found larger SOC stocks under no-
411 till compared with conventional tillage in the topsoil, but no significant differences in total SOC stocks in these
412 two tillage systems in soil profiles to 60 cm depth.
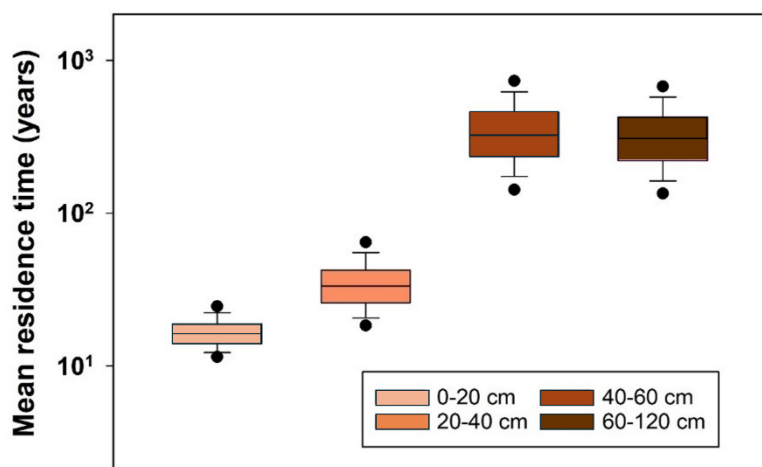
Figure 7. Distributions of mean residence times for SOM calculated in the sensitivity analysis for four depths in the soil profiles of production area PO4 in east-central Sweden. Horizontal lines show median values, the box defines the inter-quartile range, error bars define 10th and 90th percentiles and solid symbols indicate 5th and 95th percentiles.

413

Table 5. Parameter sensitivity (NRC = normalized regression coefficients)

Parameter		NRC
k_o	Decomposition rate constant (old OM)	-0.833
F_p	Physical protection factor	-0.695
A_a	Microbial energy limitation factor	0.606
HI	Harvest index	-0.513
Y	Crop Yield	0.401
ε	OM retention coefficient	0.329
f_{bg}	Fraction of NPP allocated below-ground	0.291
k_y	Decomposition rate constant (young OM)	-0.174
f_{clay}	Clay content	0.128
f_{inc}	Fraction of above-ground residues incorporated	0.127
k_{till}	Tillage transfer coefficient	-0.045
w_s	Factor for soil strength effects on root distribution	0.035
D_{95}	Root depth	-0.023
ψ_{mic}	Pressure head defining micropore region	-0.015
c	Root depth distribution factor	-0.009

4   Concluding remarks

We presented here a novel parsimonious or "minimalist" model that simulates the emergent effects of soil texture and soil structure on C stocks and turnover rates in soil profiles by mimicking two of the key processes involved in C stabilization (i.e. physical protection and microbial energy limitation). Parameters controlling these processes were also found to be among the most sensitive in the model. However, the decomposition rate constant for old microbial-processed OM, k_o was the most sensitive parameter in the model. Although k_o should be considered as a lumped parameter reflecting the influence of various processes, the available experimental evidence suggests that the strength of adsorption and OM-mineral interactions controlling the bioavailability of the substrate (i.e. chemical protection) should be the most important factor underlying its variation (e.g. Lehmann and Kleber, 2015; Mathieu et al., 2015; Doetterl et al., 2015). The development of pedotransfer approaches (van Looy et al., 2017) to estimate k_o using soil properties such as clay content and clay mineralogy, pH and Al and Fe oxides (e.g. Mathieu et al., 2015; Rasmussen et al., 2018; Fukumasu et al., 2021) would therefore be helpful in supporting predictive model applications at larger scales.

The comparisons of model simulations with local- and regional-scale data confirm that it shows promise. Despite equifinality, the parameters regulating decomposition in the model could be identified within reasonably narrow ranges using data from a long-term field experiment with three treatments characterized by strongly contrasting OM inputs for more than 50 years. Ideally, the model should now be further tested at multiple sites using data from long-term field experiments, including comparisons of alternative cropping systems and tillage management (i.e. no-till vs. conventional systems).

Competing interests

The contact author has declared that none of the authors has any competing interests.

References

Ahrens, B., Braakhekke, M., Guggenberger, G., Schrumpf, M., Reichstein, M.: Contribution of sorption, DOC transport and microbial interactions to the ^{14}C age of a soil organic carbon profile: Insights from a calibrated process model, Soil. Biol. Biochem., 88, 390-402, https://doi.org/10.1016/j.soilbio.2015.06.008, 2015.

Andrén, O., Kätterer, T.: ICBM: the introductory carbon balance model for exploration of soil carbon balances, Ecol. Appl., 7, 1226-1236, https://doi.org/10.2307/2641210, 1997.

Balesdent, J., Mariotti, A.: Natural ^{13}C abundance as a tracer for studies of soil organic matter dynamics, Soil. Biol. Biochem., 19, 25-30, https://doi.org/10.1016/0038-0717(87)90120-9, 1987.

Batjes, N.: Total carbon and nitrogen in the soils of the world, Eur. J. Soil Sci., 47, 151-163, https://doi.org/10.1111/ejss.12114_2, 1996.

Baveye, P., Schnee, L., Boivin, P., Laba, M., Radulovich, R.: Soil organic matter research and climate change: merely re-storing carbon versus restoring soil functions, Front. Environ. Sci., 8:579904, https://doi.org/10.3389/fenvs.2020.579904, 2020.

Beven, K.: A manifesto for the equifinality thesis, J. Hydrol., 320, 18-36, https://doi.org/10.1016/j.jhydrol.2005.07.007, 2006.

Beven, K., Binley, A.: GLUE: 20 years on, Hydrol. Process., 28, 5897-5918, https://doi.org/10.1002/hyp.10082, 2014.

Bolinder, M., Janzen, H., Gregorich, E., Angers, D., VandenBygaart, A.: An approach for estimating net primary productivity and annual carbon inputs to soil for common agricultural crops in Canada, Agric. Ecosyst. Environ., 118, 29-42, https://doi.org/10.1016/j.agee.2006.05.013, 2007.

Braakhekke, M., Beer, C., Hoosbeek, M., Reichstein, M., Kruijt, B., Schrumpf, M., Kabat, P.: SOMPROF: A vertically explicit soil organic matter model, Ecol. Model., 222, 1712-1730, https://doi.org/10.1016/j.ecolmodel.2011.02.015, 2011.

Braakhekke, M., Beer, C., Schrumpf, M., Ekici, A., Ahrens, B., Hoosbeek, M., Kruijt, B., Kabat, P., Reichstein, M.: The use of radiocarbon to constrain current and future soil organic matter turnover and transport in a temperate forest, J. Geophys. Res-Biogeo., 119, 372–391, The use of radiocarbon to constrain current and future soil organic matter turnover and transport in a temperate forest, https://doi.org/10.1002/2013JG002420, 2014.

Braakhekke, M., Wutzler, T., Beer, C., Kattge, J., Schrumpf, M., Ahrens, B., Schoning, I., Hoosbeek, M., Kruijt, B., Kabat, P., Reichstein, M.: Modeling the vertical soil organic matter profile using Bayesian parameter estimation, Biogeosciences, 10, 399–420, https://doi.org/10.5194/bg-10-399-2013, 2013.

Brooks, R.H. and Corey, A.T.: Hydraulic Properties of Porous Media and Their Relation to Drainage Design. Trans. ASAE, 7, 26-28, https://doi.org/10.13031/2013.40684, 1964.

Button, E., Pett-Ridge, J., Murphy, D., Kuzyakov, Y., Chadwick, D., Jones, D.: Deep-C storage: Biological, chemical and physical strategies to enhance carbon stocks in agricultural subsoils, Soil. Biol. Biochem., 170, 108697, https://doi.org/10.1016/j.soilbio.2022.108697, 2022.

Camino-Serrano, M., Guenet, B., Luyssaert, S., Ciais, P., Bastrikov, V., De Vos, B., Gielen, B., Gleixner, G., Jornet-Puig, A., Kaiser, K., Kothawala, D., Lauerwald, R., Peñuelas, J., Schrumpf, M., Vicca, S., Vuichard,

N., Walmsley, D., Janssens, I.: ORCHIDEE-SOM: modeling soil organic carbon (SOC) and dissolved organic carbon (DOC) dynamics along vertical soil profiles in Europe, Geosci. Model Dev., 11, 937-957, https://doi.org/10.5194/gmd-11-937-2018, 2018.

Campbell, E., Paustian, K.: Current developments in soil organic matter modeling and the expansion of model applications: a review, Environ. Res. Lett., 10, 123004, https://doi.org/10.1016/j.gca.2021.05.035, 2015.

Chen, S., Zou, J., Hu, Z., Lu, Y.: Temporal and spatial variations in the mean residence time of soil organic carbon and their relationship with climatic, soil and vegetation drivers, Global Planet. Change, 195, 103359, https://doi.org/10.1016/j.gloplacha.2012.10.006, 2020.

Coucheney, E., Kätterer, T., Meurer, K.H.E., Jarvis, N.: Improving the sustainability of arable cropping systems by modifying root traits: a modelling study for winter wheat, Eur. J. Soil Sci., 75, e13524, https://doi.org/10.1111/ejss.13524, 2024.

Dechow, R., Franko, U., Kätterer, T., Kolbe, H.: Evaluation of the RothC model as a prognostic tool for the prediction of SOC trends in response to management practices on arable land, Geoderma, 337, 463-478, https://doi.org/10.1016/j.geoderma.2018.10.001, 2019.

Derrien, D., Barré, P., Basile-Doelsch, I., Cécillon, L., Chabbi, A., Crème, A., Fontaine, S., Henneron, L., Janot, N., Lashermes, G., Quénéa, K., Rees, F., Dignac, M-F. : Current controversies on mechanisms controlling soil carbon storage: implications for interactions with practitioners and policy-makers. A review, Agron. Sustain. Dev., 43:21, https://doi.org/10.1007/s13593-023-00876-x, 2023.

Doetterl, S., Stevens, A., Six, J., Merckx, R., Van Oost, K., Casanova Pinto, M., Casanova-Katny, A., Muñoz, C., Boudin, M., Zagal Venegas, E., Boeckx, P.: Soil carbon storage controlled by interactions between geochemistry and climate, Nat. Geosci., 8, 780-783, https://doi.org/10.1038/ngeo2516, 2015.

Don, A., Rödenbeck, C., Gleixner, G.: Unexpected control of soil carbon turnover by soil carbon concentration, Environ. Chem. Lett., 11, 407-413, https://doi.org/10.1007/s10311-013-0433-3, 2013.

Eriksson, J., Matsson, L., Söderström, M.: Current status of Swedish arable soils and cereal crops. Data from the period 2001-2007 (in Swedish, with English summary), Report 6349, Swedish Environmental Protection Agency, Stockholm, 129 pp, https://www.slu.se/globalassets/ew/org/inst/mom/ma/akermarksinventeringen/eriksson-et-al-rapport-2010-tillstandet-i-svensk-akermark-och-groda.pdf, 2010.

Fan, J., McConkey, B., Wang, H., Janzen, H.: Root distribution by depth for temperate agricultural crops, Field Crops Res., 189, 68-74, https://doi.org/10.1016/j.fcr.2016.02.013, 2016.

Fontaine, S., Barré, P., Bdioui, N., Mary, B., Rumpel, C.: Stability of organic carbon in deep soil layers controlled by fresh carbon supply, Nature, 450, 10–14, https://doi.org/10.1038/nature06275, 2007.

Fukumasu, J., Poeplau, C. Coucheney, E., Jarvis, N., Klöffel, T., Koestel, J., Kätterer, T., Nimblad Svensson, D., Wetterlind, J., Larsbo, M.: Oxalate-extractable aluminum alongside carbon inputs may be a major determinant for organic carbon content in agricultural topsoils in humid continental climate, Geoderma, 402, 115345, https://doi.org/10.1016/j.geoderma.2021.115345, 2021.

Garsia, A., Moinet, A., Vazquez, C., Creamer, R., Moinet, G.: The challenge of selecting an appropriate soil organic carbon simulation model: A comprehensive global review and validation assessment, Global Change Biol., 29, 5760–5774, https://doi.org/10.1111/gcb.16896, 2023.

514 Haddaway, N., Hedlund, K., Jackson, L., Kätterer, T., Lugato, E., Thomsen, I., Jørgensen, H., Isberg, P-E.: How
515   does tillage intensity affect soil organic carbon? A systematic review, Environ. Evid., 6:30
516   https://doi.org/10.1186/s13750-017-0108-9, 2017.

517 Hay, R. Harvest index – a review of its use in plant-breeding and crop physiology, Ann. Appl. Biol., 126, 197-
518   216, https://doi.org/10.1111/j.1744-7348.1995.tb05015.x, 1995.

519 Hicks Pries, C., Sulman, B., West, C., O'Neill, C., Poppleton, E., Porras, R., Castanha, C., Zhui, B., Wiedemeier,
520   D., Torn, M.: Root litter decomposition slows with soil depth, Soil. Biol. Biochem., 125, 103-114,
521   https://doi.org/10.1016/j.soilbio.2018.07.002, 2018.

522 Izaurralde, R., J.R. Williams, J., McGill, W., Rosenberg, N., Quiroga Jakas, M.: Simulating soil C dynamics with
523   EPIC: Model description and testing against long-term data, Ecol. Model., 192, 362-384,
524   https://doi.org/10.1016/j.ecolmodel.2005.07.010, 2006.

525 Jackson, R., Canadell, J., Ehleringer, J., Mooney, H., Sala, O., Schulze, E.: A global analysis of root distributions
526   for terrestrial biomes, Oecologia, 108, 389-411, https://www.jstor.org/stable/4221432, 1996.

527 Jarvis, N., Coucheney, E., Lewan, E., Klöffel, T., Meurer, K., Keller, T., Larsbo, M.: Interactions between soil
528   structure dynamics, hydrological processes, and organic matter cycling: a new soil-crop model, Eur. J. Soil
529   Sci., 75, e13455, https://doi.org/10.1111/ejss.13455, 2024.

530 Jobbágy, E., Jackson, R.: The vertical distribution of soil organic carbon and its relation to climate and vegetation,
531   Ecol. Appl., 10, 423–436, https://doi.org/10.1890/1051-0761(2000)010[0423:TVDOSO]2.0.CO;2, 2000.

532 Juston, J., Andrén, O., Kätterer, T., Jansson, P-E.: Uncertainty analyses for calibrating a soil carbon balance model
533   to agricultural field trial data in Sweden and Kenya, Ecol. Model., 221, 1880-1888,
534   https://doi.org/10.1016/j.ecolmodel.2010.04.019, 2010.

535 Kätterer, T. Andrén, O., Jansson, P-E.: Pedotransfer functions for estimating plant available water and bulk density
536   in Swedish agricultural soils. Acta Agriculturae Scandinavica Section B – Soil and Plant Science, 56, 263-
537   276, https://doi.org/10.1080/09064710500310170, 2006.

538 Kätterer, T., Bolinder, M., Andrén, O., Kirchmann, H., Menichetti, L.: Roots contribute more to refractory soil
539   organic matter than above-ground crop residues, as revealed by a long-term field experiment, Agric.
540   Ecosyst. Environ., 141, 184-192, https://doi.org/10.1016/j.agee.2014.11.003, 2011.

541 Kätterer, T., Eckersten, H., Andrén, O., Pettersson, R.: Winter wheat biomass and nitrogen dynamics under
542   different fertilization and water regimes: application of a crop growth model, Ecol. Model., 102, 301-314,
543   https://doi.org/10.3390/agronomy14010110, 1997.

544 Keyvanshokouhi, S., Cornu, S., Lafolie, F., Balesdent, J., Guenet, B., Moitrier, N., Moitrier, N., Nougier, C., Finke,
545   P.: Effects of soil process formalisms and forcing factors on simulated organic carbon depth-distributions
546   in soils, Sci. Total Environ., 652, 523-537, https://doi.org/10.1016/j.scitotenv.2018.10.236, 2019.

547 Killham, K., Amato, M., Ladd, J.: Effect of substrate location in soil and soil pore-water regime on carbon turnover,
548   Soil. Biol. Biochem., 25, 57-62, https://doi.org/10.1016/0038-0717(93)90241-3, 1993.

549 Klöffel, T., Barron, J., Nemes, A., Giménez, D., Jarvis, N.: Soil, climate, time and site factors as drivers of soil
550   structure evolution in agricultural soils from a temperate-boreal region, Geoderma, 442, 116772,
551   https://doi.org/10.1016/j.geoderma.2024.116772, 2024.

552 Kravchenko, A., Negassa, W., Guber, A., Rivers, M.: Protection of soil carbon within macro-aggregates depends
553   on intra-aggregate pore characteristics, Sci. Rep., 5, 16261, https://doi.org/10.1038/srep16261, 2015.

Lehmann, J., Kleber, M.: The contentious nature of soil organic matter, Nature, 528, 60-68, https://doi.org/10.1038/nature16069, 2015.

Le Noë, J., Manzoni, S., Abramoff, R., Bölscher, T., Bruni, E., Cardinael, R., Ciais, P., Chenu, C., Clivot, H., Derrien, D., Ferchaud, F., Garnier, P., Goll, D., Lashermes, G., Martin, M., Rasse, D., Rees, F., Sainte-Marie, J., Salmon, E., Schiedung, M., Schimel, J., Wieder, W., Abiven, S., Barré, P., Cécillon, L., Guenet, B.: Soil organic carbon models need independent time-series validation for reliable prediction, Commun. Earth Environ., 4:158, https://doi.org/10.1038/s43247-023-00830-5, 2023.

Luo, Z., Wang, E., Sun, O.: Uncertain future soil carbon dynamics under global change predicted by models constrained by total carbon measurements, Ecol. Appl., 27, 1001-1009, https://doi.org/10.1002/eap.1504, 2017.

Mathieu, J., Hatté, C., Balesdent, J., Parent, E.: Deep soil carbon dynamics are driven more by soil type than by climate: a worldwide meta-analysis of radiocarbon profiles, Global Change Biol., 21, 4278-4292, https://doi.org/10.1111/gcb.13012, 2015.

Meurer, K., Chenu, C., Coucheney, E., Herrmann, A., Keller, T., Kätterer, T., Nimblad Svensson, D., Jarvis, N.: Modelling dynamic interactions between soil structure and the storage and turnover of soil organic matter, Biogeosciences, 17, 5025-5042, https://doi.org/10.5194/bg-17-5025-2020, 2020.

Meurer, K., Haddaway, N., Bolinder, M., Kätterer, T.: Tillage intensity affects total SOC stocks in boreo-temperate regions only in the topsoil – A systematic review using an ESM approach, Earth-Sci. Rev., 177, 613-622, https://doi.org/10.1016/j.earscirev.2017.12.015, 2018.

Paustian, K., Lehmann, J., Ogle, S., Reay, D., Robertson, G., Smith, P.: Climate-smart soils, Nature, 532, 49-57, https://doi.org/10.1038/nature17174, 2016.

Persson, J., Kirchmann, H.: Carbon and nitrogen in arable soils as affected by supply of N fertilizers and organic manures, Agric. Ecosyst. Environ., 51, 249-255, https://doi.org/10.1016/0167-8809(94)90048-5, 1994.

Poeplau, C., Don, A., Schneider, F.: Roots are key to increasing the mean residence time of organic carbon entering temperate agricultural soils. Global Change Biol., 27, 4921–4934, 2021.

Poeplau, C., Jacobs, A., Don, A., Vos, C., Schneider, F., Wittneibel, M., Tiemeyer, B., Heidkamp, A., Prietz, R., Flesse, H.: Stocks of organic carbon in German agricultural soils – key results of the first comprehensive inventory, J. Soil Sci. Plant Nutr., 183, 665-681, https://doi.org/10.1002/jpln.202000113, 2020.

Poeplau, C., Kätterer, T., Bolinder, M., Börjesson, G., Berti, A., Lugato, E.: Low stabilization of aboveground crop residue carbon in sandy soils of Swedish long-term experiments, Geoderma, 237/238, 246-255, https://doi.org/10.1016/j.geoderma.2014.09.010, 2015.

Pold, G., MacDonald, E., Braun S., Herrmann, A. M.: Soil and vegetation property data from the Ultuna R3-RAM56 long-term soil amendment experiment, 1956-2023, Data in Brief, 59, 111350, https://doi.org/10.1016/j.dib.2025.111350, 2025.

Rasmussen, C., Heckman, K., Wieder, W., Keiluweit, M., Lawrence, C., Berhe, A., Blankinship, J., Crow, S., Druhan, J., Hicks Pries, C., Marin-Spiotta, E., Plante, A., Schädel, C., Schimel, J., Sierra, C., Thompson, A., Wagai, R.: Beyond clay: towards an improved set of variables for predicting soil organic matter content, Biogeochemistry, 137, 297-306, https://doi.org/10.1007/s10533-018-0424-3, 2018.

Rasse, D., Rumpel, C., Dignac, M. : Is soil carbon mostly root carbon? Mechanisms for a specific stabilization, Plant Soil, 269, 341-356, https://doi.org/10.1007/s11104-004-0907-y, 2005.

Riley, W., Maggi, F., Kleber, M., Torn, M., Tang, J., Dwivedi, D., Guerry, N.: Long residence times of rapidly decomposable soil organic matter: application of a multi-phase, multi-component, and vertically resolved model (BAMS1) to soil carbon dynamics, Geosci. Model Dev., 7, 1335–1355, https://doi.org/10.5194/gmd-7-1335-2014, 2014.

Ruamps, L., Nunan, N., Chenu, C.: Microbial biogeography at the soil pore scale, Soil. Biol. Biochem., 43, 280-286, https://doi.org/10.1016/j.soilbio.2010.10.010, 2011.

Rumpel, C., Kögel-Knabner, I.: Deep soil organic matter-a key but poorly understood component of terrestrial C cycle, Plant Soil, 338, 143–158, https://doi.org/10.1007/s11104-010-0391-5, 2011.

Salomé, C., Nunan, N., Pouteau, V., Lerch, T., Chenu, C.: Carbon dynamics in topsoil and in subsoil may be controlled by different regulatory mechanisms, Global Change Biol., 16, 416-426, https://doi.org/10.1111/j.1365-2486.2009.01884.x, 2010.

Saltelli, A., Annoni, P.: How to avoid a perfunctory sensitivity analysis, Environ. Model. Softw., 25, 1508-1517, https://doi.org/10.1016/j.envsoft.2010.04.012, 2010.

Sanaullah, M., Chabbi, A., Leifeld, J., Bardoux, G., Billou, D., Rumpel, C.: Decomposition and stabilization of root litter in top- and subsoil horizons: what is the difference?, Plant Soil 338, 127–141, https://doi.org/10.1007/s11104-010-0554-4, 2011.

Schenk, H.J., Jackson, R.: The global biogeography of roots, Ecol. Monogr., 72, 311-328, https://doi.org/10.1890/0012-9615(2002)072[0311:TGBOR]2.0.CO;2, 2002.

Schiedung, H., Tilly, N., Hütt, C., Welp, G., Brüggemann, N., Amelung, W.: Spatial controls of topsoil and subsoil organic carbon turnover under C3–C4 vegetation change, Geoderma, 303, 44-51, https://doi.org/10.1016/j.geoderma.2017.05.006, 2017.

Sierra, C., Ahrens, B., Bolinder, M., Braakhekke, M., von Fromm, S., Kätterer, T., Luo, Z., Parvin, N., Wang, G.: Carbon sequestration in the subsoil and the time required to stabilize carbon for climate change mitigation, Global Change Biol., https://doi.org/10.1111/gcb.17153, 2024.

Sierra, C., Hoyt, A., He, Y., Trumbore, S.: Soil organic matter persistence as a stochastic process: age and transit time distributions of carbon in soils, Glob. Biogeochem. Cycles, 32, 1574–1588, https://doi.org/10.1029/2018GB005950, 2018.

Sleutel, S., De Neve, S., Beheydt, D., Li, C., Hofman, G.: Regional simulation of long-term organic carbon stock changes in cropland soils using the DNDC model: 1. Large-scale model validation against a spatially explicit data set, Soil Use Manag., 22, 342-351, https://doi.org/10.1111/j.1475-2743.2006.00045.x, 2006.

Smerald, A., Rahimi, J., Scheer, C.: A global dataset for the production and usage of cereal residues in the period 1997-2021, Sci. Data, 10, Article 685, https://doi.org/10.1038/s41597-023-02587-0, 2023.

Smith, P., Lutfalla, S., Riley, W., Torn, M., Schmidt, M., Soussana, J-F.: The changing faces of soil organic matter research, Eur. J. Soil Sci., 69, 23-30, https://doi.org/10.1111/ejss.12500, 2018.

Strong, D., de Wever, H., Merckx, R., Recous, S.: Spatial location of carbon decomposition in the soil pore system, Eur. J. Soil Sci., 55, 739-750, https://doi.org/10.1111/j.1365-2389.2004.00639.x, 2004.

Van Looy K., Bouma J., Herbst M., Koestel J., Minasny B., Mishra U., Montzka C., Nemes A., Pachepsky Y., Padarian J., Schaap M., Tóth B., Verhoef A., Vanderborght J., van der Ploeg M., Weihermüller L., Zacharias S., Zhang Y., Vereecken H.: Pedotransfer functions in Earth system science: challenges and perspectives, Rev. Geophys., https://doi.org/10.1002/2017RG000581, 2017.

634 Wutzler, T., Reichstein, M.: Priming and substrate quality interactions in soil organic matter models,
635   Biogeosciences, 10, 2089-2103, https://doi.org/10.5194/bg-10-2089-2013, 2013.

636 Yagasaki, Y., Shirato, Y.: Assessment on the rates and potentials of soil organic carbon sequestration in
637   agricultural lands in Japan using a process-based model and spatially explicit land-use change inventories
638   – Part 1: Historical trend and validation based on nation-wide soil monitoring, Biogeosciences, 11, 4429-
639   4442, https://doi.org/10.5194/bg-11-4429-2014, 2014.

640 Yu, L., Ahrens, B., Wutzler, T., Marion Schrumpf, M., Zaehle, S.: Jena Soil Model (JSM v1.0; revision 1934): a
641   microbial soil organic carbon model integrated with nitrogen and phosphorus processes, Geosci. Model
642   Dev., 13, 783–80, https://doi.org/10.5194/gmd-13-783-2020, 2020.

5   Complementary information

Highlights

- We outline a simple phenomenological model of soil organic carbon (SOC) turnover in a soil profile
- The model predicts effects of soil aggregation and microbial energy limitation on SOC persistence
- The model is tested using SOC data from treatments with varying C input in a long-term field trial
- The most influential parameters were identified in a sensitivity and uncertainty analysis

Running title: A simple model of SOC turnover in a soil profile

Keywords: aggregation, physical protection, microbial energy limitation, model, sensitivity

Acknowledgments

The work described in this paper was funded by the EU EJP SOIL project MaxRootC ("Optimizing roots for sustainable crop production in Europe – pure cultures and cover crops") under the H2020 Grant agreement number 862695 and by the Swedish Research Council for Sustainable Development (FORMAS, grant 2022-00214). Maintenance of the Ultuna Long-Term Field Experiment (RAM-56) is funded by the Faculty of Natural Resources and Agricultural Sciences at the Swedish University of Agricultural Sciences (SLU, Sweden). We would also like to thank Lorenzo Menichetti (formerly at SLU Department of Ecology, now at LUKE, The Natural Resources Institute of Finland) and Frédéric Rees (INRAE, France) for helpful discussions on this work.

Data availability statement

The data used in the model application to the Ultuna Long-term Organic Matter trial can be obtained by following the link to an on-line repository given in Pold et al. (2025). The model, which is built in the modelling software tool STELLA, as well as the data underlying the plots and the EXCEL data file developed for the sensitivity analysis can be made available on request.

Authors email, ORCID-ID and contributions

Email addresses and ORCID-ID in brackets:

elsa.coucheney@slu.se (0000-0001-5988-2085)

anke.herrmann@slu.se (0000-0002-6273-1234)

nicholas.jarvis@slu.se (0000-0001-6725-6762)

AUTHOR CONTRIBUTIONS

ELSA COUCHENEY: Conceptualization; methodology; writing – original draft; writing - review and editing.

ANKE HERRMANN: Investigation; data curation; funding acquisition; writing - review and editing.

NICHOLAS JARVIS: Conceptualization; formal analysis; funding acquisition; methodology; project administration; writing – original draft; writing - review and editing.